RNA (2002), *8*:626–636. Cambridge University Press. Printed in the USA.

DOI: 10.1017.S1355838202020022

Yeast Pescadillo is required for multiple activities during 60S ribosomal subunit synthesis

MARLENE OEFFINGER,[1] ANTHONY LUENG,[2] ANGUS LAMOND,[2] and DAVID TOLLERVEY[1]

[1]Wellcome Trust Centre for Cell Biology, University of Edinburgh, Edinburgh, EH9 3JR, United Kingdom
[2]Wellcome Trust Biocentre, University of Dundee, Dundee, United Kingdom

ABSTRACT

The Pescadillo protein was identified via a developmental defect and implicated in cell cycle progression. Here we report that human Pescadillo and its yeast homolog (Yph1p or Nop7p) are localized to the nucleolus. Depletion of Nop7p leads to nuclear accumulation of pre-60S particles, indicating a defect in subunit export, and it interacts genetically with a tagged form of the ribosomal protein Rpl25p, consistent with a role in subunit assembly. Two pre-rRNA processing pathways generate alternative forms of the 5.8S rRNA, designated $5.8S_L$ and $5.8S_S$. In cells depleted for Nop7p, the $27SA_3$ pre-rRNA accumulated, whereas later processing intermediates and the mature $5.8S_S$ rRNA were depleted. Less depletion was seen for the $5.8S_L$ pathway. TAP-tagged Nop7p coprecipitated precursors to both $5.8S_L$ and $5.8S_S$ but not the mature rRNAs. We conclude that Nop7p is required for efficient exonucleolytic processing of the $27SA_3$ pre-rRNA and has additional functions in 60S subunit assembly and transport. Nop7p is a component of at least three different pre-60S particles, and we propose that it carries out distinct functions in each of these complexes.

Keywords: nucleolus; pre-rRNA; ribosome; RNA processing

INTRODUCTION

Most steps in ribosome synthesis take place within the nucleolus, a specialized subnuclear structure. During ribosome synthesis, a complex processing pathway converts a large pre-rRNA to the mature 18S, 5.8S, and 25S/28S rRNAs (see Fig. 1B). In addition, the mature rRNA sequences within the pre-RNA undergo extensive covalent nucleotide modification and assembly with the 80 ribosomal proteins. More than 80 nonribosomal proteins that are required for ribosome synthesis have been identified by genetic and biochemical approaches in yeast (see Kressler et al., 1999; Venema & Tollervey, 1999; Warner, 2001). Biochemical analyses in human cells have identified an even larger number of nucleolar proteins (Anderson et al., 2002), although in most cases, their function in ribosome synthesis has not yet been directly addressed. Subdomains of the human nucleolus can be identified microscopically. Transcription of the rDNA is believed to occur at the boundaries of the fibrillar centers with initial processing and preribosome assembly occurring in the associated dense fibrillar component (DFC) regions. Later processing and assembly of the pre-ribosomes occurs in the surrounding granular component (GC) of the nucleolus (see, e.g., Shaw & Jordan, 1995; Scheer & Hock, 1999; Lyon & Lamond, 2000). Most analyses of subnuclear structure have been performed on vertebrates and plants, but similar structures are present in yeast (Leger-Silvestre et al., 1997, 1999).

During pre-rRNA processing, the $27SA_2$ pre-rRNA can be processed by two alternative pathways (Henry et al., 1994; see Fig. 1B). In the major pathway, the pre-rRNA is cleaved at site A_3 by RNase MRP, forming the $27SA_3$ pre-rRNA. Subsequent exonuclease digestion to site B_{1S} requires the two known $5' \rightarrow 3'$ exonucleases, Xrn1p and Rat1p, and generates the 5′ end of the $27SB_S$ pre-rRNA and mature $5.8S_S$ rRNA (Henry et al., 1994). An alternative, poorly understood, pathway processes the pre-rRNA at site B_{1L}, the 5′ end of the $27SB_L$ pre-rRNA. Both 27SB pre-rRNAs are subsequently processed, by apparently identical pathways, to generate the mature 25S rRNA and either the $5.8S_S$ or $5.8S_L$ rRNAs (see Fig. 1). The ratio between the two forms of 5.8S shows some variation between strains, but around 75–80% of the population is normally made up of $5.8S_S$, which is 8 nt shorter than $5.8S_L$. Similar 5′ heterogeneity is seen for 5.8S rRNA from many other Eukaryotes, including humans, *Xenopus*, *Drosophila*, and plants (Henry et al., 1994), sug-

Reprint requests to: David Tollervey, Wellcome Trust Centre for Cell Biology, University of Edinburgh, Edinburgh, EH9 3JR, United Kingdom; e-mail: d.tollervey@ed.ac.uk.

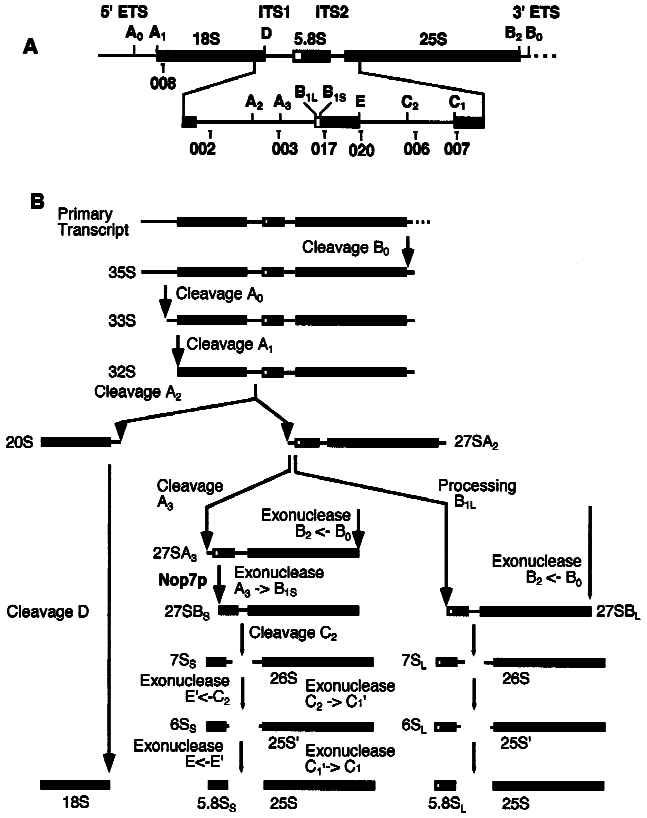

FIGURE 1. Pre-rRNA processing in *S. cerevisiae*. **A:** Structure and processing sites of the 35S pre-rRNA. This precursor contains the sequences for the mature 18S, 5.8S, and 25S, which are separated by the two internal transcribed spacers ITS1 and ITS2 and flanked by the two external transcribed spacers 5′ETS and 3′ETS. The positions of the oligonucleotide probes utilized in northern hybridization and primer extension analyses are indicated. **B:** Pre-rRNA processing pathway. The 35S pre-rRNA is generated by 3′ cleavage at site B_0. 35S is then cleaved at site A_0 to produce the 33S pre-rRNA, which is rapidly cleaved at site A_1, producing the 32S pre-rRNA. 32S is cleaved at site A_2, separating the precursors to the 40S and 60S subunits, the 20S and $27SA_2$ pre-rRNAs, respectively. $27SA_2$ is processed via two alternative pathways. In the major pathway, cleavage at site A_3 by RNase MRP produces $27SA_3$, which is then trimmed to site B_{1S} by the 5′ to 3′ exonucleases Rat1p and Xrn1p, producing the $27SB_S$ pre-rRNA. Alternatively, $27SA_2$ can be processed to $27SB_L$ by an undetermined mechanism. $27SB_S$ and $27SB_L$ are matured to the 5.8S and 25S by identical pathways. Trimming to site B_2 generates the mature 3′ end of the 25S rRNA. Cleavage at site C_2 and exonuclease digestion by Rat1p and Xrn1p generates the 5′ end of mature 25S. The 3′ end of the 5.8S is generated by 3′ to 5′ exonuclease digestion from site C_2 to E. For reviews on pre-rRNA processing and *trans*-acting factors see Kressler et al. (1999), Lafontaine and Tollervey (2001), and Venema and Tollervey (1999).

gesting that the existence of two processing pathways is both conserved and functionally significant.

The Pescadillo gene was initially identified in Zebrafish as the site of retrovirus insertion, which resulted in defects in embryonic development (Allende et al., 1996). Pescadillo mRNA showed widespread expression in developing mouse embryo brain with increased protein levels in replicating cells (Kinoshita et al., 2001). Protein levels were also increased in malignant cells (Kinoshita et al., 2001), possibly related to previous reports of increased nucleolar size and ribosome synthesis in such cells. Pescadillo was localized to the nucleolus in Hela cells (Kinoshita et al., 2001) and the *Schizosaccharomyces pombe* homolog, SPBC19F5.05c, was also found to be nucleolar in a high throughput screen for subcellular localization of GFP fusion proteins (Ding et al., 2000). While this work was in progress, characterization of the yeast Pescadillo homolog Yph1p/Nop7p (YGR103w) was reported. YGR103w was originally published under the name of *YPH1* (Kinoshita et al., 2001), but has been designated as *NOP7* by the *Saccharomyces* genetic database. Nop7p is essential for viability and two temperature-sensitive (ts) lethal mutant alleles were reported to block growth at different steps in the cell-cycle; *yph1-24* led to arrest in G1, whereas the *yph1-45* allele caused G2 arrest (Kinoshita et al., 2001). G1 arrest is expected for mutations defective in ribosome synthesis, which are unable to pass the "Start" checkpoint control, but G2 arrest would not normally be predicted for a ribosome synthesis defect. In addition, Pescadillo was observed to contain a BRCT domain (Haque et al., 2000), which was originally identified in the breast and ovarian cancer gene BRCA1 and has been identified in several proteins involved in cell-cycle checkpoints and DNA repair (reviewed in Bork et al., 1997). Based on these observations, Pescadillo and Yph1p/Nop7p were proposed to perform some cell-cycle specific function.

A proteomic analysis of the human nucleolus identified 271 putative nucleolar proteins including Pescadillo (Anderson et al., 2002), the nucleolar localization of which was confirmed by YFP-tagging. A database search clearly identified YGR103w as the probable yeast homolog and we therefore analyzed its role in ribosome synthesis. While this work was in progress, the purification of a precursor to the 60S ribosomal subunit was reported that made use of a tagged form of Nop7p (Harnpicharnchai et al., 2001). This analysis did not, however, describe the effects of depletion of Yph1p/Nop7p on pre-rRNA processing or ribosome synthesis. Here we show that Nop7p is required for formation of $27SB_S$, and therefore of the mature $5.8S_S$ rRNA, from the $27SA_3$ pre-rRNA and has additional functions in subunit assembly or export.

RESULTS

Human Pescadillo and yeast Nop7p are localized to the nucleolus

A proteomic analysis of purified human nucleoli identified 271 proteins, one of which was Pescadillo (Anderson et al., 2002). To confirm this localization, an eYFP-Pescadillo construct was expressed in Hela cells by transient transfection (Fig. 2A). Comparison of the localization of eYFP-Pescadillo (shown in green; Fig. 2A4) to a DIC image (Fig. 2A1) showed its predominant lo-

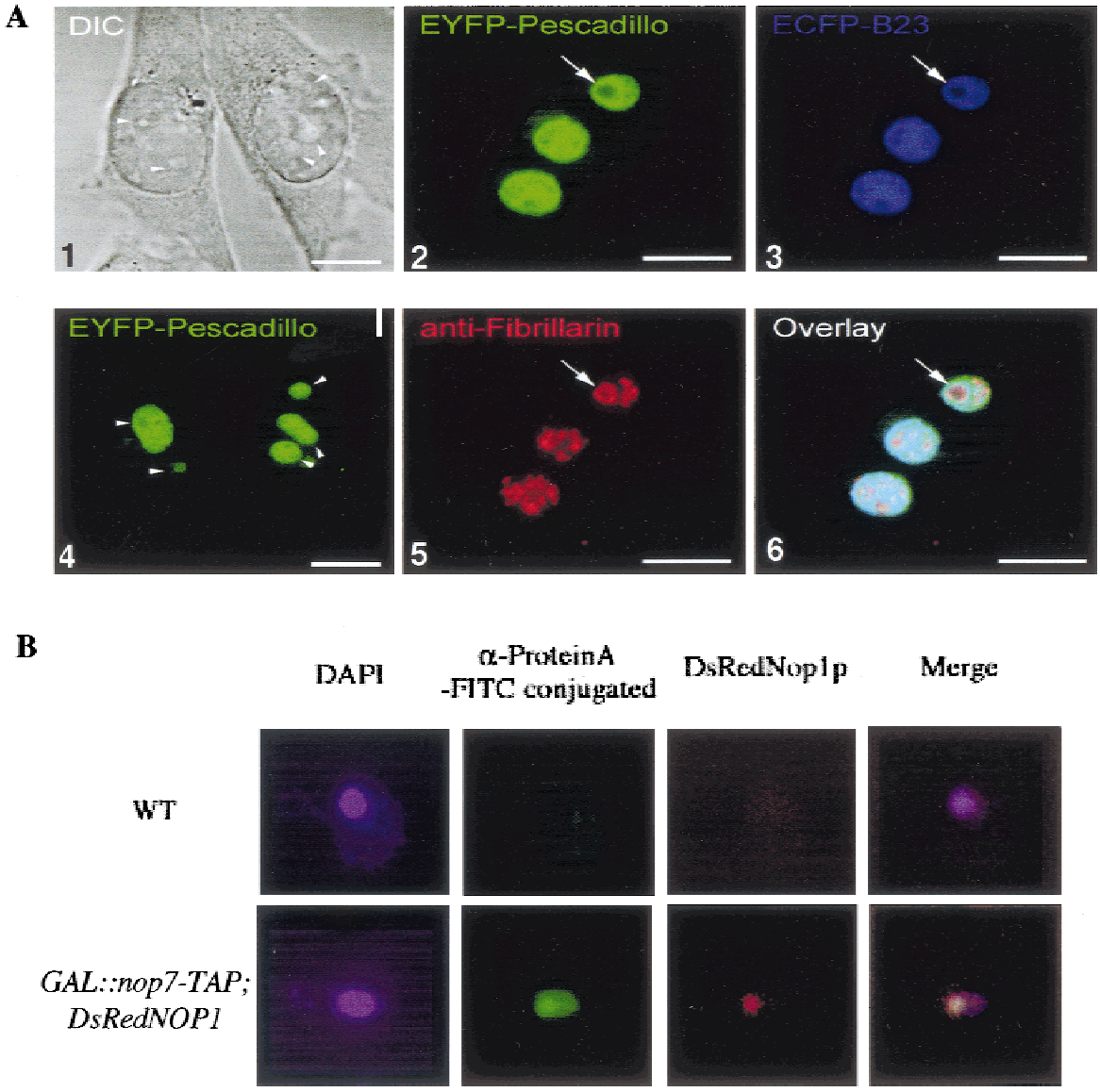

FIGURE 2. Nucleolar localization of Pescadillo and Nop7p. **A:** Localization of human Pescadillo compared with known nucleolar markers. (1, 4) Hela cells were fixed 16 h after transfection with EYFP-Pescadillo. Comparison to the DIC image (1) shows localization of eYFP-Pescadillo (4; green) to nucleoli (arrowheads). 2, 3, 5, and 6: As markers for subnucleolar distribution, the EYFP-Pescadillo transfected cells (2; green) were cotransfected with the granular component protein ECFP-B23 (3; blue) and decorated with antibodies directed against the dense fibrillar component (DFC) protein fibrillarin (5; red). Scale bar = 5 μm. **B:** Localization of Nop7p. The *GAL::nop7-TAP* strain also expressing the nucleolar marker DsRedNop1p was examined by indirect immunofluorescence using an anti-protein A antibody coupled to FITC. Also shown is the position of the nucleus visualized by DAPI staining and a wild-type control strain.

calization to nucleoli (indicated by arrowheads) with a low level of nucleoplasmic staining.

The subnucleolar distribution of eYFP-Pescadillo (Fig. 2A2) was compared to the GC marker eCFP-tagged B23/nucleophosmin (Npm1) (shown in blue; Fig. 2A3) and the DFC marker fibrillarin (shown in red; Fig. 2A5). Fibrillarin is a component of the box C+D snoRNAs (Schimmang et al., 1989) that function early in ribosome synthesis, whereas B23 is a putative assembly factor and nuclease that is believed to act later in ribosome synthesis (Biggiogera et al., 1990; Savkur & Olson, 1998). In vitro, B23 is reported to cleave a pre-rRNA reporter within ITS2 (Savkur & Olson, 1998), at a site potentially equivalent to C_2 in the yeast pre-rRNA. Fibrillarin is concentrated in the DFC whereas B23 was reported to localize to the periphery of the DFC and the GC based on immuno-EM (Biggiogera et al., 1990), consistent with a later role for B23 in nucleolar ribosome maturation. The distribution of eYFP-Pescadillo resembled that of eCFP-B23, but was distinct from that of fibrillarin. eYFP-Pescadillo and eCFP-B23 were largely excluded from the DFCs (one

of which is indicated by an arrow) and concentrated in the surrounding area, which presumably corresponds to the GC. The distribution of eYFP-Pescadillo is consistent with a late role in nucleolar ribosome synthesis.

The essential yeast protein Nop7p (YGR103w) is 40% identical to human Pescadillo. To determine whether Nop7p is also nucleolar, it was epitope tagged with a tandem-affinity purification (TAP) construct (Rigaut et al., 1999) using a one-step PCR protocol (see Materials and Methods). The tagged construct was integrated at the *NOP7* locus under the control of the *GAL10* promoter and is the only source of Nop7p. The host strain, YDL401, has reduced galactose permease activity leading to reduced *GAL* induction (Lafontaine & Tollervey, 1996). This eliminates the overexpression generally seen with *GAL*-regulated constructs and allows faster appearance of phenotypes following transfer to glucose medium. The *GAL::nop7-TAP* cells exhibited no detectable growth defect on permissive RSG medium, showing the fusion construct to be fully functional (data not shown).

To determine the location of Nop7-TAP, cells were examined by indirect immunofluorescence (Fig. 2B) using a rabbit anti-protein A and a secondary FITC-coupled goat anti-rabbit antibody to detect the protein A region of the TAP tag (Rigaut et al., 1999). As a marker for the nucleolus, a DsRed fusion with the nucleolar protein Nop1p (the yeast homolog of fibrillarin) was coexpressed as previously described (Gadal et al., 2001b), and the nucleoplasm was identified by DAPI staining. Anti-protein A preferentially decorated the nucleolus, with a weaker signal over the nucleoplasm. No cytoplasmic signal was detected. We conclude that Nop7p is localized to the nucleus with nucleolar enrichment. The significant nucleoplasmic staining would be consistent with association with late pre-ribosomes that have been released from the nucleolus (see Milkereit et al., 2001).

Yeast Nop7p is required for 60S subunit export and interacts genetically with GFP-tagged Rpl25p

To examine the possible functions of Nop7p in ribosome synthesis, its expression was placed under the control of a repressible *GAL10* promoter using a one-step PCR technique in strain YDL401 (see Materials and Methods). Growth of the *GAL::nop7* strain was not clearly different from the isogenic wild-type strain on RGS medium, but was progressively slowed following transfer to glucose medium, commencing around 6 h after transfer (Fig. 3A). The *yph1-45* allele of *NOP7* is reported to lead to a G2 arrest phenotype, consistent with a specific cell-cycle defect (Kinoshita et al., 2001). However, microscopic inspection of the *GAL::nop7* strain following transfer to glucose medium showed only the accumulation of unbudded cells, even after 24 h, indicating arrest in G1 (data not shown). This is the expected phenotype for a defect in ribosome synthesis that results in the inability to pass the "Start" checkpoint.

Several recent studies have made use of fusions between ribosomal proteins and GFP to follow the ex-

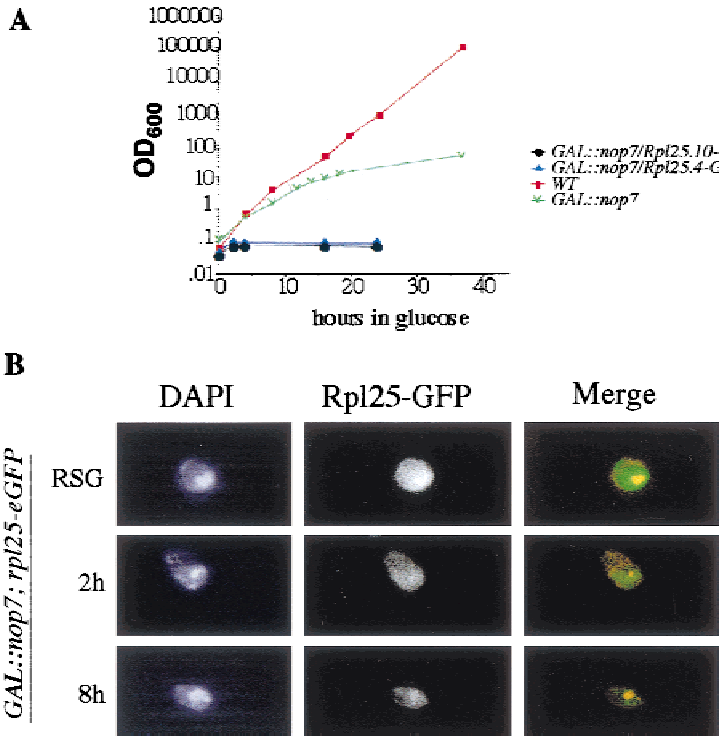

FIGURE 3. Nop7p is required for 60S subunit export and interacts genetically with GFP-tagged Rpl25p. **A:** Growth curves of *GAL::nop7* strains following transfer to glucose medium, with and without expression of Rpl25p-eGFP. Strains were pregrown in RGS medium and transferred to glucose medium for the times indicated. Strains were maintained in exponential growth by dilution with prewarmed medium. Cell densities measured by OD_{600} are shown corrected for dilution. (■) Wild-type; (∗) *GAL::nop7*; (●) *GAL::nop7*; *rpl25.10-GFP*; (▲) *GAL::nop7*; *rpl25.4-GFP*. **B:** Subcellular distribution of Rpl25-eGFP in a *GAL::nop7* strain. Rpl25-eGFP was examined by fluorescence microscopy during growth in RGS medium and following transfer to glucose medium for 2 and 8 h. The position of the nucleus was visualized by DAPI staining, which also stains the cytoplasm more weakly due to the presence of mitochondria. In the merged image, DAPI staining is shown in red and Rpl25-GFP is in green.

port of 60S ribosomal subunits from the nucleus to the cytoplasm (Stage-Zimmermann et al., 2000; Baßler et al., 2001; Gadal et al., 2001a, 2001b; Milkereit et al., 2001; Fatica et al., 2002). To look for 60S subunit export defects, Rpl25p-eGFP (Gadal et al., 2001b) was expressed from a plasmid in the wild-type and *GAL::nop7* strains. As previously reported, expression of this construct had little effect on the growth of the wild-type strain (Gadal et al., 2001b) or the *GAL::nop7* strain on galactose medium (data not shown). Unexpectedly, growth of the *GAL::nop7*/Rpl25p-eGFP strain was very rapidly inhibited following transfer to glucose medium (Fig. 3; two independent transformants are shown). These strains also express the wild-type Rpl25p, showing that the Rpl25p-eGFP fusion is dominant negative for growth in strains with a reduced level of Nop7p. The growth inhibition is much more rapid than would have been expected for a strain that is simply unable to synthesize new ribosomes (see Discussion) and we conclude that Nop7p has a role in 60S ribosomal subunit assembly.

The distribution of Rpl25p-eGFP was followed during depletion of Nop7p (Fig. 3B). During growth of the *GAL::nop7* strain on RSG medium, Rpl25-eGFP showed the normal, predominantly cytoplasmic distribution. After transfer to glucose medium for 2 h, increased nuclear staining of Rpl25-eGFP was already visible, and accumulation was strong after 8 h. The distribution of Rpl25-eGFP fluorescence matched that of DAPI staining, indicating that it was not restricted to the nucleolus. We conclude that Nop7p is required to allow the export of precursors to the 60S ribosomal subunit from the nucleoplasm to the cytoplasm.

Nop7p is required for pre-rRNA processing

The effects of depletion of Nop7p were assessed by Northern hybridization (Fig. 4), primer extension (Fig. 5), and pulse-chase labeling (Fig. 6).

Depletion of Nop7p resulted in mild accumulation of the 35S primary transcript and the appearance of low levels of the 23S RNA, but had little impact on levels of the $27SA_2$ or 20S pre-rRNAs, or the mature 18S rRNA (Fig. 4A). In contrast, the level of the 27SB pre-rRNAs was clearly reduced by 8 h after transfer to glucose medium and the mature 25S rRNA was depleted over time.

Analysis of low-molecular-weight RNAs showed progressive reduction in the levels of the 7S and 6S pre-rRNAs following transfer of the *GAL::nop7* strain to glucose medium (Fig. 4Bb). The level of the mature 5.8S was also reduced (Fig. 4Bc), and the reduction in $5.8S_S$ appeared slightly greater than for $5.8S_L$. The pre-rRNA that extends from A_2 to C_2 was not accumulated during Nop7p depletion (Fig. 4Ba), in contrast to the recently reported effects of depletion of another processing factor, Ssf1p (Fatica et al., 2002).

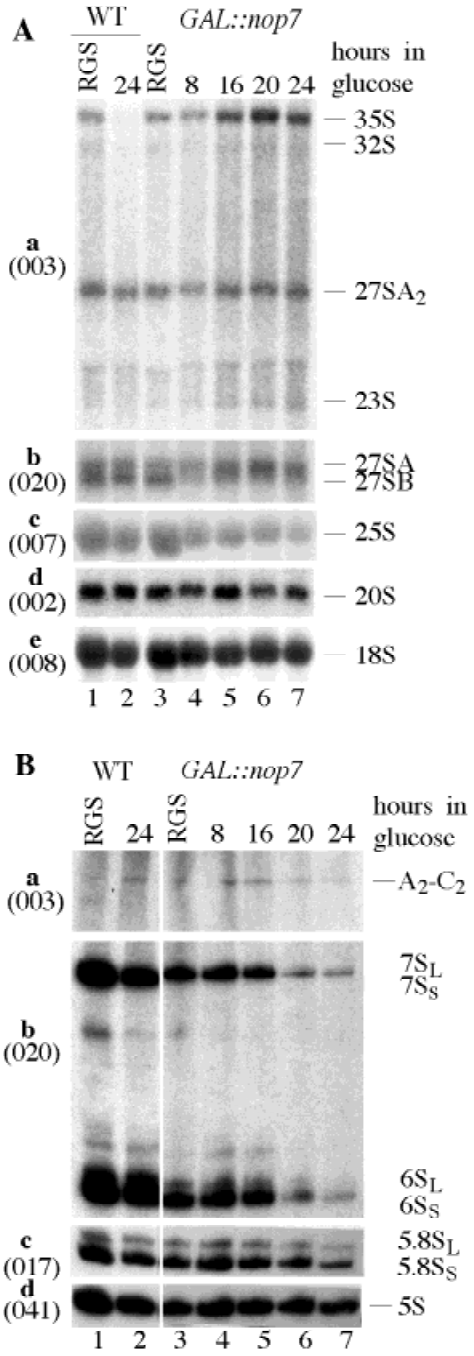

FIGURE 4. Northern analysis of the effects of Nop7p depletion on pre-rRNA processing. Lanes 1 and 2: wild-type strain in RGS medium and 24 h after transfer to glucose. Lanes 3–7: *GAL::nop7* strain in RGS medium and after transfer to glucose medium for the times indicated. **A:** (a) Hybridization of probe 003, complementary to ITS1 upstream of A_3. (b) Hybridization with probe 020, complementary to the 5.8S/ITS2 boundary. (c) Hybridization with probe 007, complementary to the 25S rRNA. (d) Hybridization with probe 002, complementary to ITS1 upstream of A_2. (e) Hybridization with probe 008, complementary to 18S rRNA. **B:** (a) Hybridization with probe 003, complementary to ITS1 upstream of A_3. (b) Hybridization with probe 020, complementary to the 5.8S/ITS2 boundary. (c) Hybridization with probe 017, complementary to 5.8S rRNA. (d) Hybridization with probe 041, complementary to 5S rRNA. RNA was separated on a 1.2% agarose/formaldehyde gel (**A**) or 8% polyacrylamide/urea gel (**B**). Probe names are indicated in parentheses on the left.

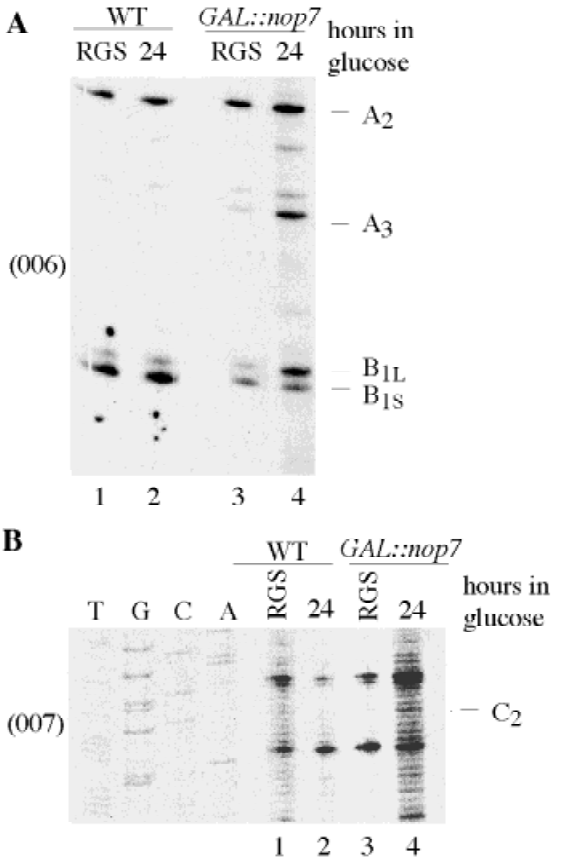

FIGURE 5. Primer extension analysis of pre-rRNA processing. Lanes 1 and 2: wild-type strain in RGS medium and 24 h after transfer to glucose medium. Lanes 3 and 4: *GAL::nop7* strain in RGS medium and 24 h after transfer to glucose medium. **A:** Primer extension using oligo 006, which hybridizes within ITS2, 3′ to site C_2. Primer extension stops at sites A_2, A_3, B_{1S}, and B_{1L} show the levels of the $27SA_2$, $27SA_3$, $27SB_L$, and $27SB_S$ pre-rRNAs, respectively. **B:** Primer extension using oligo 007, which hybridizes within 25S rRNA. The primer extension stop at C_2 shows the level of the 26S pre-rRNA.

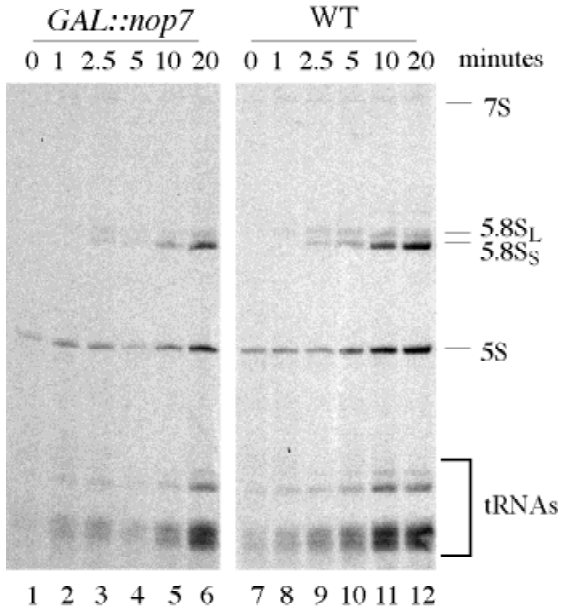

FIGURE 6. Pulse-chase analysis of rRNA synthesis. Pre-rRNA was pulse labeled with [^{3}H]uracil for 2 min at 30 °C and chased with a large excess of unlabeled uracil for the times indicated. Labeling was performed for the *GAL::nop7* strain (lanes 1–6) and a wild-type strain (lanes 7–12) 16 h after transfer to glucose medium.

$5.8S_S$ is processed from the $27SB_S$ pre-rRNA, whereas $5.8S_L$ is processed from $27SB_L$ (see Fig. 1B). To determine the levels of the 27SB species, they were analyzed by primer extension (Fig. 5A) using an oligo hybridizing within the 3′ region of ITS2 (oligo 006; see Fig. 1A). Following growth of the *GAL::nop7* strain on glucose medium, the level of $27SB_S$ was clearly reduced relative to $27SB_L$, as shown by the primer extension stops at B_{1S} and B_{1L}, respectively (Fig. 5A, lane 4). Consistent with the northern analysis, little alteration was seen in the level of $27SA_2$, as shown by the primer extension stop at site A_2. In contrast, the level of $27SA_3$, shown by the stop at site A_3, was substantially elevated. Using a primer hybridizing within the mature 25S rRNA (oligo 007; see Fig. 1A), slight accumulation was seen for the primer extension stop at site C_2, the 5′ end of the 26S pre-rRNA (Fig. 5B). This effect was weak, however, and its significance is unclear.

Pulse-chase analysis with [H^3]-uracil was performed 16 h after transfer to glucose minimal medium (Fig. 6). Comparison of the wild-type and *GAL::nop7* strains showed that accumulation of the 5.8S rRNA was mildly delayed.

Together these data show that depletion of Nop7p resulted in reduced exonuclease digestion from site A_3 to site B_{1S}. In consequence, the level of the $27SA_3$ pre-rRNA was substantially increased, whereas the $27SB_S$ pre-rRNA was depleted together with the $7S_S$ and $6S_S$ pre-rRNAs, leading to reduced accumulation of the mature $5.8S_S$ rRNA. The 5′ end of the 25S rRNA is also generated by exonuclease digestion (Geerlings et al., 2000; see Fig. 1B), but this did not appear to be strongly affected, as only a small increase was seen in the primer extension stop at site C_2. The mild effects on 35S processing are likely to be indirect, as many mutations that inhibit synthesis of 60S subunits result in partial inhibition of the early pre-rRNA processing steps (for further discussion see Venema & Tollervey, 1999).

Nop7p is associated with pre-rRNAs from both processing pathways

To determine whether Nop7p associated specifically with the $27SB_S$ branch of the processing pathway, coprecipitated RNAs were analyzed by northern analysis and primer extension. Northern hybridization (Fig. 7A,B) showed that the 27SB and 7S pre-rRNAs coprecipitated with Nop7-TAP, but were not detectably recov-

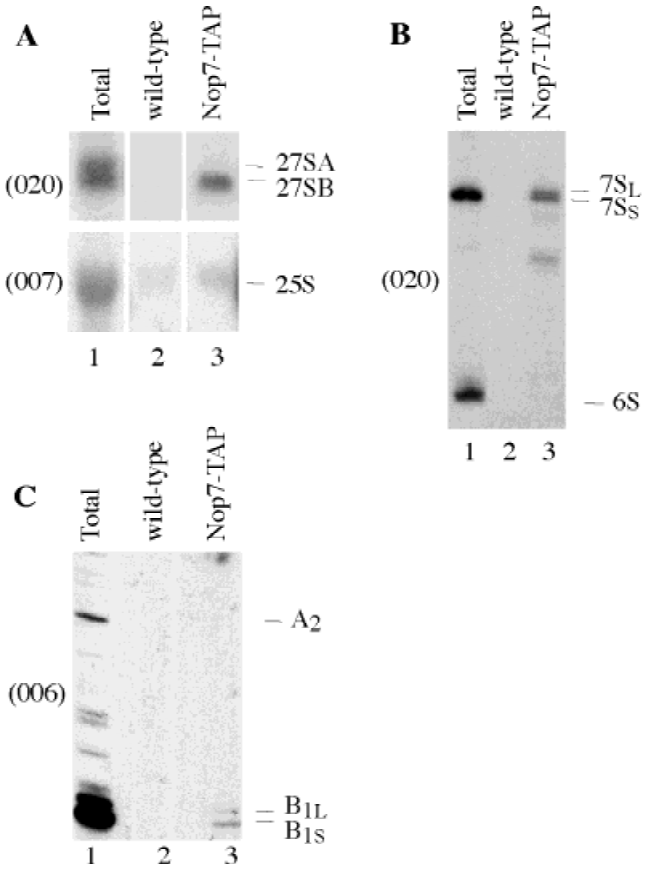

FIGURE 7. Analysis of RNAs coprecipitated with TAP-tagged Nop7p. Lane 1: Total RNA control (5 μg). Lane 2: Precipitate from a wild-type control strain. Lane 3: Precipitate from a strain expressing Nop7-TAP. **A:** Northern hybridization of high-molecular-weight RNA separated on a 1.2% agarose/formaldehyde gel. **B:** Northern hybridization of low-molecular-weight RNA separated on an 8% polyacrylamide/urea gel. **C:** Primer extension analysis. Nop7-TAP was immunoprecipitated from cell lysates using IgG agarose, with release of bound RNA–protein complexes by cleavage of the protein A linker by TEV protease. RNA was recovered from the released material, and from a mock-treated, isogenic wild-type control strain. Oligonucleotides used are indicated in parentheses. The preparation used in **C** is different from that used for **A** and gave lower recovery efficiency.

ered in the mock precipitation from the nontagged wild-type strain. In contrast, the $27SA_2$ and 6S pre-rRNAs were not detectably coprecipitated. The 25S rRNA gave the same background signal in both the wild-type and Nop7-TAP precipitates. Inspection of the original figure showed that both the $7S_L$ and $7S_S$ pre-rRNAs were coprecipitated. $27SB_L$ and $27SB_S$ cannot be resolved by northern hybridization, but primer extension from oligo 006 in ITS2 (see Fig. 1A) showed that both the $27SB_L$ and $27SB_S$ pre-RNAs were coprecipitated with Nop7-TAP (Fig. 7C).

Nop7p has a specific role in formation of the $27SB_S$ pre-rRNA but is associated with pre-rRNAs in both processing pathways, consistent with the conclusion that it has additional roles in 60S subunit assembly and export.

DISCUSSION

We show here that the yeast homolog of Pescadillo is required for the 5′ to 3′ exonuclease digestion that generates the 5′ end of the major, short form of the 5.8S rRNA. Depletion of Nop7p also resulted in strong synergistic inhibition of growth in the presence of a GFP-tagged form of ribosomal protein Rpl25p, indicating an additional role in 60S ribosome assembly. Nuclear accumulation of Rpl25-eGFP has been used as a marker for a defect in nuclear export of pre-60S ribosomal particles (ribosome export or *rix* phenotype; Gadal et al., 2001b), and this was also observed following Nop7p depletion. We conclude that Nop7p is required for a specific pre-rRNA processing step as well as correct pre-60S assembly and nuclear export.

During the course of this work, Nop7p was shown to be a component of at least three different pre-ribosomal complexes with substantially different protein composition, as well as differences in pre-rRNA components (Baßler et al., 2001; Harnpicharnchai et al., 2001; Fatica et al. 2002; see Fig. 8). These analyses allow us to propose a correlation between the pre-ribosomal particles with which Nop7p is associated and the distinct defects in ribosome synthesis that are seen on its depletion.

The earliest pre-60S particle with which Nop7p is known to be associated is pre-60S E_1. This complex is also associated with the $27SA_2$, $27SA_3$, and 27SB pre-rRNAs (Fatica et al., 2002) and it is therefore very likely that Nop7p is required for processing from $27SA_3$ to 27SB within the pre-60S E_1 particle.

A fast acting, dominant negative phenotype is associated with the expression of a GFP-tagged form of the ribosomal protein Rpl25p in strains depleted of Nop7p. The fact that expression of Rpl25-GFP is dominant in-

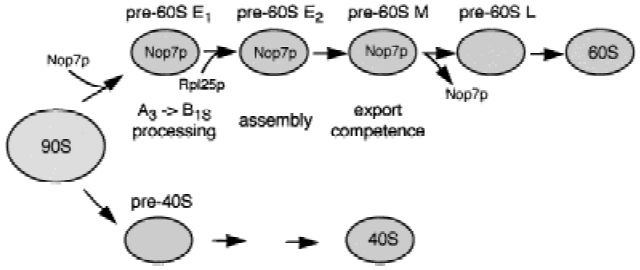

FIGURE 8. Model for the roles of Nop7p in 60S subunit biogenesis. Outline pathway of biogenesis of 60S and 40S ribosomal subunits, modified from Fatica et al. (2002). This model indicates the presence of Nop7p in three different pre-60S complexes designated E_1, E_2, and M, which can be correlated with the different functions deduced for Nop7p. Pre-60S E_1 contains the $27SA_3$ pre-rRNA, the processing of which is defective in strains lacking Nop7p. Rpl25p is not present in pre-60S E_1, but joins the pre-60S E_2 particle, and the defect in Rpl25p assembly is therefore predicted to occur at this step. The pre-60S M complex contains numerous factors required for 60S subunit export as judged by the nuclear retention of a Rpl25-GFP reporter construct, and Nop7p is likely to be required during the acquisition of export competence within this complex.

dicates that, in its presence, the wild-type Rpl25p is no longer able to support growth. Notably, the inhibition of growth was much more rapid and complete than would be expected for a strain that was simply unable to synthesize new ribosomes due to pre-rRNA processing defects. Many such mutants have been analyzed (reviewed in Venema & Tollervey, 1999) and predominantly show a gradual increase in doubling time, as preformed ribosomes are depleted by growth. The very rapid onset of growth inhibition, seen in the Nop7p-depleted strain expressing Rlp25-GFP, indicates that this does not require substantial depletion of the pre-existing ribosome pool. We speculate that production of defective subunits prevents the remaining, otherwise functional, ribosomes from carrying out efficient translation. The pre-60S E_1 complex lacks Rpl25p, which is added only to the pre-60 E_2 particle (Harnpicharnchai et al., 2001; Fatica et al., 2002). We therefore predict that the genetic interaction between *GAL::nop7* and Rpl25-GFP reflects a requirement for Nop7p in the correct assembly of Rpl25p, and perhaps other factors, with the pre-60S E_2 complex.

Several recent studies have made use of a fusion between Rpl25p and GFP to follow the export of 60S ribosomal subunits from the nucleus to the cytoplasm (Baßler et al., 2001; Gadal et al., 2001a, 2001b; Ho et al., 2000; Milkereit et al., 2001; Fatica et al., 2002). There is considerable data showing that free r-proteins do not accumulate in the absence of ribosome synthesis. The accumulation of Rlp25-GFP has therefore been taken as evidence for the accumulation of pre-ribosomal particles in the nucleoplasm, indicating a defect in their export. This assay has defined a late pre-ribosomal particle (pre-60S M in Fig. 8), all tested components of which are required for 60S subunit export. These include Nug1p, Nug2p, Noc2p, Noc3p, and Rix1p as well as Nop7p itself (Baßler et al., 2001; Gadal et al., 2001a, 2001b; Milkereit et al., 2001). Mutations in any of these proteins leads to defects in export, suggesting a requirement for the intact structure of this pre-ribosomal particle. Because multiple components of this complex are required for subunit export, we predict that export competence is established within this particle, and that this activity requires Nop7p.

Mutations in Nug1p, Nug2p, Noc2p, Noc3p, or Rix1p did not result in pre-rRNA processing defects similar to Nop7p depletion or synergistic interactions with Rpl25-GFP (Baßler et al., 2001; Milkereit et al., 2001) indicating that these are distinct activities. Moreover, Nug1-TAP did not coprecipitate $27SA_2$ or $27SA_3$ (Baßler et al., 2001; E. Petfalski & D. Tollervey, unpubl. observations) indicating that it associates with the pre-rRNA particle only after processing at these sites is complete. Depletion of a specific component of the pre-60S E_1 complex, Ssf1p, also did not interact genetically with Rpl25-GFP and did not inhibit subunit export as judged by nuclear accumulation of Rpl25-GFP (Fatica et al., 2002). We therefore propose that the roles of Nop7p in pre-rRNA processing, assembly, and export are distinct and performed within different pre-ribosomal particles (see Fig. 8).

Pescadillo is a multifunctional protein

Pescadillo was isolated as a mutation affecting embryonic development (Allende et al., 1996) and a mutant allele of the yeast gene resulted in growth arrest in G2 (Kinoshita et al., 2001), consistent with a specific defect in cell-cycle progression. Yeast Yhp1p/Nop7p is also reported to interact with Yvh1p (Sakumoto et al., 2001), a protein-tyrosine phosphatase with a postulated role in the regulation of sporulation and meiosis.

There are clear precedents for proteins that function both in cell-cycle progression and ribosome synthesis. Exit from mitosis in budding yeast requires a group of proteins, including the phosphatase Cdc14p, which down-regulate cyclin-dependent kinase activity. Cdc14p is sequestered in the nucleolus in the RENT (regulator of nucleolar silencing and telophase) complex with Sir2p and Net1p, which serves to anchor the complex (Shou et al., 1999). In addition, Net1p is required for the maintenance of normal nucleolar structure and its binding stimulates RNA polymerase I (Shou et al., 1999, 2001). These nucleolus-specific functions of Net1p can be separated genetically from its cell-cycle functions in the RENT complex. In human cells, the nucleolar p14/ARF protein binds and sequesters the negative regulator of p53 activity, Mdm2 (Tao & Levine, 1999; Weber et al., 1999; Zhang & Xiong, 1999). Free Mdm2 ubiquitinates p53 and transports it to the cytoplasm where it is degraded by the proteosome (Fuchs et al., 1998; Geyer et al., 2000), and the nucleolar sequestration of Mdm2 contributes to the inhibition of this activity by ARF. Mouse Pescadillo was identified by its up-regulation in cells lacking p53 (Kinoshita et al., 2001), but other interactions with the p53 system have not been reported.

The available data suggest that yeast Nop7p may function both in ribosome synthesis and in cell-cycle regulation. Whether its role in the cell cycle involves other protein components of the pre-ribosomal particles or a different set of interactions remains to be determined.

MATERIALS AND METHODS

Strains

Growth and handling of *Saccharomyces cerevisiae* were by standard techniques. *GAL*-regulated strains were pregrown in RGS medium, containing 2% raffinose, 2% galactose, and 2% sucrose, and harvested at intervals following a shift to medium containing 2% glucose. Strains for pulse-chase analysis were pregrown in minimal RGS medium lacking uracil and shifted to minimal glucose medium lacking uracil. Strains for

immunofluorescence studies were grown in minimal glucose medium lacking leucine.

Yeast strains used and constructed in this study are listed in Table 1. Conditional mutants under the control of the repressible *GAL10* promoter were generated by one-step PCR strategy in the strains YDL401 and BMA64 (Lafontaine & Tollervey, 1996). Transformants were selected for HIS+ prototrophy and screened by PCR. TAP-tagged strains were constructed by one-step PCR strategy in the GAL-mediated strain *GAL::nop7* (Rigaut et al., 1999). Transformants were screened by immunoblotting and PCR.

TAP-tagged strains were transformed with pUN100Ds RedNOP1 (kindly provided by E. Hurt and U. Heidelberg) to allow ready identification of the nucleolus, and pYEplac195-L25-eGFP to look at nuclear export of 60S ribosomal subunits.

For construction of eYFP-PES, complementary DNA of human Pescadillo gene (GI:2194202) was isolated by PCR amplification from Marathon-Ready Hela cDNA library (Clontech) using specific primers with *Bgl*II and *Eco*RI restriction sites attached to the 5′ and 3′ primer, respectively. The amplified fragment was subsequently cloned to the *Bgl*II-*Eco*RI fragment of eYFP-C1 and verified by DNA sequencing.

RNA extraction, northern hybridization, and primer extension

RNA was extracted as described previously (Tollervey & Mattaj, 1987). For high-molecular-weight RNA analysis, 7 μg of total RNA were separated on a 1.2% agarose gel containing formaldehyde and transferred for northern hybridization as described previously (Tollervey, 1987). Standard 6% or 8% acrylamide-8 M urea gels were used to analyze low-molecular-weight RNA species and primer extension reactions. Primer extensions were performed as described previously (Beltrame & Tollervey, 1992) on 5 μg of total RNA using primers 007 and 006.

For pre-rRNA and rRNA analysis the following oligonucleotides were used:

002: 5′-GCTCTTTGCTCTTGCC;
003: 5′-TGTTACCTCTGGGCCC;
006: 5′-AGATTAGCCGCAGTTGG
007: 5′-CTCCGCTTATTGATATGC;
008: 5′-CATGGCTTAATCTTTGAGAC;
017: 5′-GCGTTGTTCATCGATGC;
020: 5′-TGAGAAGGAAATGACGCT;
041: 5′-CTACTCGGTCAGGCTC.

Immunofluorescence

For localization of yeast Nop7p, cells were grown in selective medium to midexponential phase, fixed by incubation in 4% (v/v) formaldehyde for 30 min at 25 °C, and spheroplasted. Immunofluorescence was then performed as described previously (Grandi et al., 1993; Bergès et al., 1994). Protein A fusions were detected with a rabbit anti-Protein A antibody (Sigma) and a secondary goat anti-rabbit antibody coupled to FITC (Sigma) at 1:1,000 and 1:200 dilutions, respectively. To stain nuclear DNA, DAPI was included in the mounting medium (Vectashield, Vector Laboratories). Cells were viewed on a Zeiss Axioscop microscope.

Cells containing pYE195-Rpl25-eGFP were grown in SD-LEU to midexponential phase, fixed in 4% (v/v) formaldehyde for 30 min, and pelleted. Cells were resuspended in 100 mM KH_2Ac/K_2HAc/1.1 M sorbitol and mounted onto slides using moviol, containing DAPI. To detect Rpl25-eGFP in vivo in the fluorescence microscope, the GFP-signal was examined in the fluorescein channel of a Zeiss Axioscop microscope (Hurt et al., 1999). Pictures were obtained with SmartCapture VP.

The localization of eYFP-Pescadillo was determined after transient transfection into Hela cells. EYFP-PES and eCFP-B23 were cotransfected for 6 h using Effectene (Quiagen) according to the manufacturer's protocol and fixed after 42 h using 3.7% paraformaldehyde in CSK buffer. Cells were permeabilized and decorated with antibodies against dense fibrillar component marker fibrillarin (72B9) and the granular component marker B23 (anti-B23). Cells were imaged using a Zeiss LSM410 confocal microscope or a Zeiss DeltaVision Restoration microscope (Applied Precision, Inc.). Images presented here are maximal projections of the entire nuclear fluorescence.

Immunoprecipitation of *GAL::nop7*-TAP

For immunoprecipitation of *GAL::nop7*-TAP, cells were grown in YPgal to $OD_{600} = 2$ and lysed in buffer A (150 mM KAc, 20 mM Tris-Ac, pH 7.5, 5 mM MgAc) with 1 mM DTT, 0.5% Triton X-100, 2.5 mM vanadyl-ribonucleoside complexes (VRC), and 5 mM PMSF (phenylmethylsulphonylfluoride) at

TABLE 1. Yeast strains used and constructed in this study.

Strain	Genotype	Reference
YDL401	MATa *his3Δ200 leu2Δ1 trp1 ura3-52 gal2 galΔ108*	Lafontaine & Tollervey, 1996
YMO1	as YDL401 but *GAL10::nop7-HIS3*	This work
YMO2	as YDL401 but *GAL10::nop7-TAP-TRP1*	This work
YMO3	as YMO2 but pUN100-DsRed*nop1* LEU1	This work
YMO4	as YMO1 but pRS315-*Rpl25*-eGFP	This work
BMA64	MATa *ade2-1 his3-11,-15 leu2-3,-112 trp1Δ, ura3-1*	F. Lacroute
YMO5	as BMA64 but pA3*ura*3	This work
YMO6	as BMA64 but *GAL10::nop7*, pA3*ura*3	This work
YCA31	as YDL401 but *GAL10::prot.A-RRP4*, *RRP6:(KI)TRP1*	Allmang et al., 1999
GAL::DOB1	MATa *ura3-1 ade2-1 his3-11,-15 leu2-3,-112 trp1-1* Dob1::HIS3MX6 +[pAS24-*DOB1*]	de la Cruz et al., 1998

4 °C using glass beads (Sigma). Immunoprecipitation with rabbit IgG agarose beads and subsequent TEV cleavage were performed as described (Rigaut et al., 1999). RNA was extracted with buffer AE/phenol-chloroform, ethanol precipitated (Schmitt et al., 1990), and analyzed by northern hybridization and primer extension.

Pulse-chase labeling experiments

Pulse-chase labeling of pre-rRNA was performed as previously described (Tollervey et al., 1993) using 100 μCi [5,6-^{3}H]uracil (Amersham) for 2 min at 30 °C. Unlabeled uracil was added to a final concentration of 240 μgmL^{-1}. Samples (1 mL) were taken, transferred to microcentrifuge tubes at room temperature, and spun for 10 s at full speed in an Eppendorf centrifuge. Cell pellets were frozen in liquid N_2. Total RNA was extracted with buffer AE/phenol-chloroform and ethanol precipitated (Schmitt et al., 1990). [H^3]-labeled pre-rRNA and rRNA was resolved on 1.2% agarose gels for high-molecular-weight RNAs and 8% acrylamide-8 M urea gels for low-molecular-weight RNAs. RNA was transferred to Hybond-N$^+$ Nylon membranes (Amersham), dried, and exposed to X-ray film for 10 days at −80 °C with an intensifying screen.

ACKNOWLEDGMENTS

M.O. was the recipient of a Darwin Trust Fellowship and A.L. was the recipient of a Studentship from the Croucher Foundation of Hong Kong. A.L. and D.T. are Wellcome Trust Principal Fellows. This work was supported by the Wellcome Trust.

Received December 10, 2001; returned for revision January 3, 2002; revised manuscript received February 22, 2002

REFERENCES

Allende ML, Amsterdam A, Becker T, Kawakami K, Gaiano N, Hopkins N. 1996. Insertional mutagenesis in Zebrafish identifies two novel genes, Pescadillo and dead eye, essential for embryonic development. *Genes & Dev 10*:3141–3155.

Allmang C, Kufel J, Chanfreau G, Mitchell P, Petfalski E, Tollervey D. 1999. Functions of the exosome in rRNA, snoRNA and snRNA synthesis. *EMBO J 18*:5399–5410.

Anderson J, Lyon CE, Fox A, Leung AKL, Lam YW, Steen H, Mann M, Lamond AI. 2002. Directed proteomic analysis of the human nucleolus. *Current Biology 12*:1229–1231.

Baßler J, Grandi P, Gadal O, Leßmann T, Petfalski E, Tollervey D, Lechner J, Hurt E. 2001. Identification of a 60S pre-ribosomal particle that is closely linked to nuclear export. *Mol Cell 8*:517–529.

Beltrame M, Tollervey D. 1992. Identification and functional analysis of two U3 binding sites on yeast pre-ribosomal RNA. *EMBO J 11*:1531–1542.

Bergès T, Petfalski E, Tollervey D, Hurt EC. 1994. Synthetic lethality with fibrillarin identifies NOP77p, a nucleolar protein required for pre-rRNA processing and modification. *EMBO J 13*:3136–3148.

Biggiogera M, Burki K, Kaufmann SH, Shaper JH, Gas N, Amalric F, Fakan S. 1990. Nucleolar distribution of proteins B23 and nucleolin in mouse preimplantation embryos as visualized by immunoelectron microscopy. *Development 110*:1263–1270.

Bork P, Hofmann K, Bucher P, Neuwald AF, Altschul SF, Koonin EV. 1997. A superfamily of conserved domains in DNA damage-responsive cell cycle checkpoint proteins. *FASEB J 11*:68–76.

de la Cruz J, Kressler D, Tollervey D, Linder P. 1998. Dob1p (Mtr4p) is a putative ATP-dependent RNA helicase required for the 3′ end formation of 5.8S rRNA in *Saccharomyces cerevisiae*. *EMBO J 17*:1128–1140.

Ding DQ, Tomita Y, Yamamoto A, Chikashige Y, Haraguchi T, Hiraoka Y. 2000. Large-scale screening of intracellular protein localization in living fission yeast cells by the use of a GFP-fusion genomic DNA library. *Genes Cells 5*:169–190.

Fatica A, Cronshaw AD, Dlakic M, Tollervey D. 2002. Ssf1p prevents premature processing of an early pre-60S ribosomal particle. *Mol Cell 9*:341–351.

Fuchs SY, Adler V, Buschmann T, Wu X, Ronai Z. 1998. Mdm2 association with p53 targets its ubiquitination. *Oncogene 17*:2543–2547.

Gadal O, Strauss D, Braspenning J, Hoepfner D, Petfalski E, Philippsen P, Tollervey D, Hurt E. 2001a. A nuclear AAA-type ATPase (Rix7p) is required for biogenesis and nuclear export of 60S ribosomal subunits. *EMBO J 20*:3695–3704.

Gadal O, Strauss D, Kessl J, Trumpower B, Tollervey D, Hurt E. 2001b. Nuclear export of 60s ribosomal subunits depends on Xpo1p and requires a nuclear export sequence-containing factor, Nmd3p, that associates with the large subunit protein Rpl10p. *Mol Cell Biol 21*:3405–3415.

Geerlings TH, Vos JC, Raue HA. 2000. The final step in the formation of 25S rRNA in *Saccharomyces cerevisiae* is performed by 5′ → 3′ exonucleases. *RNA 6*:1698–1703.

Geyer RK, Yu ZK, Maki CG. 2000. The MDM2 RING-finger domain is required to promote p53 nuclear export. *Nat Cell Biol 2*:569–573.

Grandi P, Doyl V, Hurt EC. 1993. Purification of NSP1 reveals complex formation with 'GLFG' nucleoporins and a novel nuclear pore protein NIC96. *EMBO J 12*:3061–3071.

Haque J, Boger S, Li J, Duncan SA. 2000. The murine Pes1 gene encodes a nuclear protein containing a BRCT domain. *Genomics 70*:201–210.

Harnpicharnchai P, Jakovljevic J, Horsey E, Miles T, Roman J, Rout M, Meagher D, Imai B, Guo Y, Brame CJ, Shabanowitz J, Hunt DF, Woolford JL. 2001. Composition and functional characterization of yeast 66s ribosome assembly intermediates. *Mol Cell 8*:505–515.

Henry Y, Wood H, Morrissey JP, Petfalski E, Kearsey S, Tollervey D. 1994. The 5′ end of yeast 5.8S rRNA is generated by exonucleases from an upstream cleavage site. *EMBO J 13*:2452–2463.

Ho JH, Kallstrom G, Johnson AW. 2000. Nmd3p is a Crm1p-dependent adapter protein for nuclear export of the large ribosomal subunit. *J Cell Biol 151*:1057–1066.

Hurt E, Hannus S, Schmelzl B, Lau D, Tollervey D, Simos G. 1999. A novel in vivo assay reveals inhibition of ribosomal nuclear export in ran-cycle and nucleoporin mutants. *J Cell Biol 144*:389–401.

Kinoshita Y, Jarell AD, Flaman JM, Foltz G, Schuster J, Sopher BL, Irvin DK, Kanning K, Kornblum HI, Nelson PS, Hieter P, Morrison RS. 2001. Pescadillo, a novel cell cycle regulatory protein abnormally expressed in malignant cells. *J Biol Chem 276*:6656–6665.

Kressler D, Linder P, de La Cruz J. 1999. Protein *trans*-acting factors involved in ribosome biogenesis in *Saccharomyces cerevisiae*. *Mol Cell Biol 19*:7897–7912.

Lafontaine D, Tollervey D. 1996. One-step PCR mediated strategy for the construction of conditionally expressed and epitope tagged yeast proteins. *Nucleic Acids Res 24*:3469–3472.

Lafontaine DL, Tollervey D. 2001. The function and synthesis of ribosomes. *Nat Rev Mol Cell Biol 2*:514–520.

Leger-Silvestre I, Noaillac-Depeyre J, Faubladier M, Gas N. 1997. Structural and functional analysis of the nucleolus of the fission yeast Schizosaccharomyces pombe. *Eur J Cell Biol 72*:13–23.

Leger-Silvestre I, Trumtel S, Noaillac-Depeyre J, Gas N. 1999. Functional compartmentalization of the nucleus in the budding yeast *Saccharomyces cerevisiae*. *Chromosoma 108*:103–113.

Lyon CE, Lamond AI. 2000. The nucleolus. *Curr Biol 10*:R323.

Milkereit P, Gadal O, Podtelejnikov A, Trumtel S, Gas N, Petfalski E, Tollervey D, Mann M, Hurt E, Tschochner H. 2001. Maturation and intranuclear transport of pre-ribosomes requires Noc proteins. *Cell 105*:499–509.

Rigaut G, Shevchenko A, Rutz B, Wilm M, Mann M, Seraphin B. 1999. A generic protein purification method for protein complex characterization and proteome exploration. *Nat Biotechnol 17*:1030–1032.

Sakumoto N, Yamashita H, Mukai Y, Kaneko Y, Harashima S. 2001. Dual-specificity protein phosphatase Yvh1p, which is required for vegetative growth and sporulation, interacts with yeast Pescadillo homolog in *Saccharomyces cerevisiae*. *Biochem Biophys Res Commun 289*:608–615.

Savkur RS, Olson MO. 1998. Preferential cleavage in pre-ribosomal RNA byprotein B23 endoribonuclease. *Nucleic Acids Res 26*: 4508–4515.

Scheer U, Hock R. 1999. Structure and function of the nucleolus. *Curr Opin Cell Biol 11*:385–390.

Schimmang T, Tollervey D, Kern H, Frank R, Hurt EC. 1989. A yeast nucleolar protein related to mammalian fibrillarin is associated with small nucleolar RNA and is essential for viability. *EMBO J 8*:4015–4024.

Schmitt ME, Brown TA, Trumpower BL. 1990. A rapid and simple method for preparation of RNA from *Saccharomyces cerevisiae*. *Nucleic Acids Res 18*:3091–3092.

Shaw PJ, Jordan EG. 1995. The nucleolus. *Annu Rev Cell Dev Biol 11*:93–121.

Shou W, Sakamoto KM, Keener J, Morimoto KW, Traverso EE, Azzam R, Hoppe GJ, Feldman RM, DeModena J, Moazed D, Charbonneau H, Nomura M, Deshaies RJ. 2001. Net1 stimulates RNA polymerase I transcription and regulates nucleolar structure independently of controlling mitotic exit. *Mol Cell 8*:45–55.

Shou W, Seol JH, Shevchenko A, Baskerville C, Moazed D, Chen ZW, Jang J, Shevchenko A, Charbonneau H, Deshaies RJ. 1999. Exit from mitosis is triggered by Tem1-dependent release of the protein phosphatase Cdc14 from nucleolar RENT complex. *Cell 97*:233–244.

Stage-Zimmermann T, Schmidt U, Silver PA. 2000. Factors affecting nuclear export of the 60S ribosomal subunit in vivo. *Mol Biol Cell 11*:3777–3789.

Tao W, Levine AJ. 1999. P19(ARF) stabilizes p53 by blocking nucleo-cytoplasmic shuttling of Mdm2. *Proc Natl Acad Sci USA 96*: 6937–6941.

Tollervey D. 1987. A yeast small nuclear RNA is required for normal processing of pre-ribosomal RNA. *EMBO J 6*:4169–4175.

Tollervey D, Lehtonen H, Jansen R, Kern H, Hurt EC. 1993. Temperature-sensitive mutations demonstrate roles for yeast fibrillarin in pre-rRNA processing, pre-rRNA methylation, and ribosome assembly. *Cell 72*:443–457.

Tollervey D, Mattaj IW. 1987. Fungal small nuclear ribonucleoproteins share properties with plant and vertebrate U-snRNPs. *EMBO J 6*:469–476.

Venema J, Tollervey D. 1999. Ribosome synthesis in *Saccharomyces cerevisiae*. *Ann Rev Gen 33*:261–311.

Warner JR. 2001. Nascent ribosomes. *Cell 107*:133–136.

Weber JD, Taylor LJ, Roussel MF, Sherr CJ, Bar-Sagi D. 1999. Nucleolar Arf sequesters Mdm2 and activates p53. *Nat Cell Biol 1*:20–26.

Zhang Y, Xiong Y. 1999. Mutations in human ARF exon 2 disrupt its nucleolar localization and impair its ability to block nuclear export of MDM2 and p53. *Mol Cell 3*:579–591.